Academic Journal of Science and Technology
ISSN: 2771-3032 | Vol. 9, No. 3, 2024

Prediction of the Modal Parameters of The Spindle System in High-speed Dry Hobbing Machine with Thermal Effects

Chao Zhang*, Benjie Li, Changlin Yu, Huangshuai Li, Yingcai Zhu

School of Mechatronic Engineering, Southwest Petroleum University, Chengdu, 610500, China
* Corresponding author: Zhang Chao (Email: ZC_0123@126.com)

Abstract: High-speed dry hobbing is an advanced green machining technology for gears. However, thermal issues in the machine tools become serious under the high cutting speed and dry cutting conditions, which result in a nonlinear evolution of the machine tool dynamics, and finally affect the hobbing stability. In view of this, introducing the hob spindle system as the object, this paper intends to investigate the influence of time-varying temperatures on the modal parameters based on the modal tests. Then, a temperature-dependent modal parameters prediction model based on the multi-output Gaussian process regression (MOGPR) is proposed. The experimental results indicated that the modal parameters of the spindle system vary obviously with changing thermal states. The natural frequencies for the first and third modes increased with the temperature rise, while the variation of the natural frequency for the second mode was insignificant. The damping ratios for the first three modes showed a decreasing trend with the temperature rise. The constructed MOGPR model has the capability to effectively predict the modal parameters with the time-varying thermal effects, which can provide a support to build the temperature-dependent hobbing stability boundaries.

Keywords: High-speed dry hobbing, Spindle system, Time-varying thermal effects, Modal parameters, Multi-output Gaussian Process regression.

1. Introduction

High-speed dry hobbing process has become a key technology for the green machining of industrial gears due to its advantages of high productivity, low cost, and outstanding environmental benefits [1]. However, compared with the traditional wet hobbing, high-speed dry hobbing has more serious thermal problems, such as large temperature field gradient, strong thermal stress, large thermal deformation [2]. At the same time, the time- varying thermal effect in the high-speed dry hobbing process will significantly affect the machine tool dynamics, and finally affect the hobbing stability [3, 4]. This is one of the main problems restricting the machine tool reliability, machining quality and productivity. Therefore, it is necessary to study the machine tool dynamics under the time-varying thermal effects in the high - speed dry hobbing process.

Numerous efforts have been made to study the thermal issues in high-speed dry hobbing machine tools, such as the heat transfer characteristics [5], thermal balance modeling and control methods [6, 7, 8], thermal error compensation strategies [9]. It is found from the above researches that the high-speed dry hobbing machine tool has a complex thermal behaviors. Compared with the other components such as the machine tool columns and bed, the spindle system has a faster thermal response and then can reflect the thermal characteristics of the machine tool to a large extent [10]. Therefore, many attentions have been focused on the thermal characteristics of the spindle system. Ma et al. [11] carried out a simulation and experimental research on the thermal characteristics of a high-speed motorized spindle system by considering the thermo-structural coupling effect and revealed the temperature field distribution and thermal deformation characteristics of the high-speed motorized spindle system. Yan et al. [12] estimated the temperatures of each part of the spindle system by using the convolution of the temperatures of the measured heat source and the thermal response function. Based on this, a thermal error modeling method was developed. Ge and Ding [13] proposed a thermal error control method for the high-speed motorized spindle based on the thermal deformation balance principle, which can effectively reduce the thermal error of the spindle. Grama et al. [14] proposed a cooling method of the motorized spindle system based on the cooling trigger model, which is beneficial to ensure the thermal stability of the spindle motor and bearing and control the thermal deformation of the spindle. Zheng et al. [15] established a comprehensive thermal network model of high-speed spindle bearings by comprehensively considering the external air convection and lubricating oil cooling and lubrication. The above researches are of great significance for improving the thermal stability of the spindle system and alleviating the thermal deformation of the spindle. However, the dynamic characteristics of the spindle system under the time-varying thermal effects have not been studied.

During the high-speed dry hobbing process, the uneven temperature rises and thermal deformations of the bearing, motor and other components of the spindle system are bound to alter the bearing preloads, which finally result in the variations of the spindle system dynamics [16]. Zhang et al. [17] established a quasi-static five-degree- of-freedom dynamic model for the angular contact ball bearing of the spindle system and revealed the changes of bearing preloads under non-uniform temperature rise. Stein et al. [18] proposed a state-space model for monitoring the thermal preload of the bearings in the high-speed machine tools. Lin et al. [19] established a thermo-mechanical-dynamic coupling model of a motorized electric spindle and demonstrated that the thermal

effects have a significant effect on the stiffness of the spindle. The above researches show that the thermal-induced bearing preload is the main source changing the spindle dynamics during the operation process of the spindle system. However, the current researches mainly focused on the effects of thermal-induced bearing preload on the bearing stiffness characteristics. The evolution of the spindle system dynamics under the time-varying thermal effects has not been revealed and the relationship between the thermal effect and spindle system dynamics has not been quantified.

In view of this, this paper intends to study the dynamic behaviors of the spindle system in a high-speed dry hobbing machine tool. Wherein the variations in the modal parameters are taken as the indicators to characterize the evolution of the spindle system dynamics. First, the time-varying temperatures of the spindle system were measured during the continuous high-speed dry hobbing process. Moreover, the modal parameters of the spindle system were identified using the extracted free vibration responses from the operation vibration signals. Subsequently, a multi-output Gaussian process regression (MOGPR) model is constructed considering the correlations within the modal parameters. Finally, the established MOGPR model is trained and tested to quantify the mapping relationship between the modal parameters and temperature variables. The developed temperature-dependent modal parameters prediction model can provide a support for the hobbing stability analysis under the time-varying thermal effect during the high-speed dry hobbing process.

2. Experiment

In order to study the dynamic characteristic evolution behavior of the spindle system of the high-speed dry hobbing machine under the time-varying thermal effect, based on the thermal mode experiment, the mapping relationship between the modal parameters of the spindle system and the time - varying temperature during operation was studied. Based on YE3115CNC high-speed dry hobbing machine, the experimental platform for thermal mode analysis of the spindle system was built, Fig. 1. The parameters of hob used in the experiment are as follows: diameter - 75mm, normal modulus - 1.95mm, number of slots - 16, number of heads - 1, Angle of thread rise -2.17º (LH), base material - S390, coating material - AlCrN. The parameters of the gear workpiece to be machined are: number of teeth -52, helix Angle - 27º (LH), normal pressure Angle -20º, tooth width - 15.55mm, gear material -20CrMoH.

First of all, for the hob spindle and workpiece shaft, the impact modal experiment was carried out, as shown in Fig 1 (a), to analyze the influence behavior and degree of thermal state change on their dynamic characteristics. LC-02 impact hammer is used to excite the hob and the workpiece in the initial state and the thermal balance state respectively, and PCB 356A16 three-axis acceleration sensor is used to pick up the response of the hob and the workpiece. In this paper, all the data in the experiment process were collected synchronously by the dynamic data acquisition system developed on the basis of NI 9231 and NI 9214 acquisition cards and LabVIEW software platform. The sampling frequency of force hammer signal and acceleration signal was 5120Hz.

In order to further reveal the influence of time- varying temperature on dynamic characteristics in the process of high-speed dry hobbing, and quantify the mapping relationship between time- varying temperature and modal parameters, operational modal experiment analysis was carried out on the continuous machining process of high-speed dry hobbing, as shown Fig. 1 (b). During the experiment, the speed of the hob was 950r/min and the feed rate was 3.0mm/rev. The high-speed dry hobbing process uses compressed air with a temperature of 19℃ for auxiliary cooling, and the internal motor of the spindle uses cooling water with a temperature of 25℃ for circulating cooling.

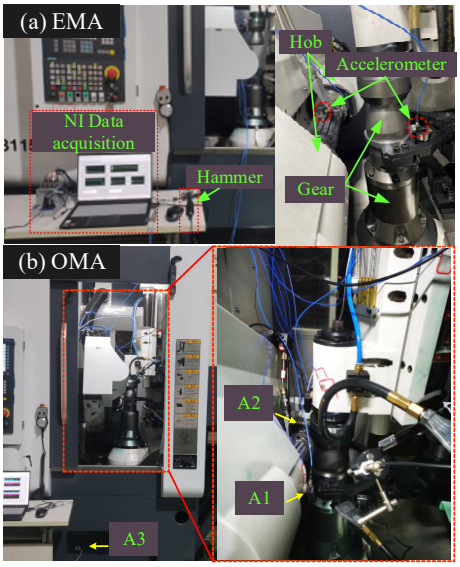

Figure 1. Experimental setup of machine tool

In the process of high-speed dry hobbing continuous machining, since it is impossible to install an acceleration sensor on the hob, a three-axis acceleration sensor is installed at the spindle end bearing seat (A1) and the spindle head (A2) respectively to pick up the spindle vibration signal during operation. In addition, a three-axis acceleration sensor is installed at the bed (A3), which is used as a reference point to extract modal parameters during operation. OMEGA EXTT-K24-SLE thermocouple temperature sensors are arranged in the spindle motor housing (T1), the spindle middle bearing seat (T2) and the hob end bearing seat (T3, T4), respectively, which are used to collect time-varying temperature data of the spindle system during high-speed dry hobbing.

3. Thermal Mode Experimental Analysis

Based on the impact mode experiment, estimate the frequency response function of hob and workpiece in the initial state and thermal balance state before processing for the experimental data after window processing, as shown in Fig. 2. It can be seen from the figure that from the initial state to the thermal balance state, the frequency response function of hob and workpiece moves to the right as a whole. It indicates that the change of thermal state changes the dynamic characteristics of the hob and the workpiece. In addition, the frequency response function at the hob moves more, while the frequency response function at the workpiece moves less, indicating that the time-varying thermal effect during high-speed dry hobbing has a greater impact on the dynamic characteristics of the hob spindle, while the dynamic characteristics of the workpiece shaft are almost unaffected by the time-varying thermal effect during the machining process. Therefore, this paper mainly studies the influence of

the time - varying thermal effect on the hob spindle system.

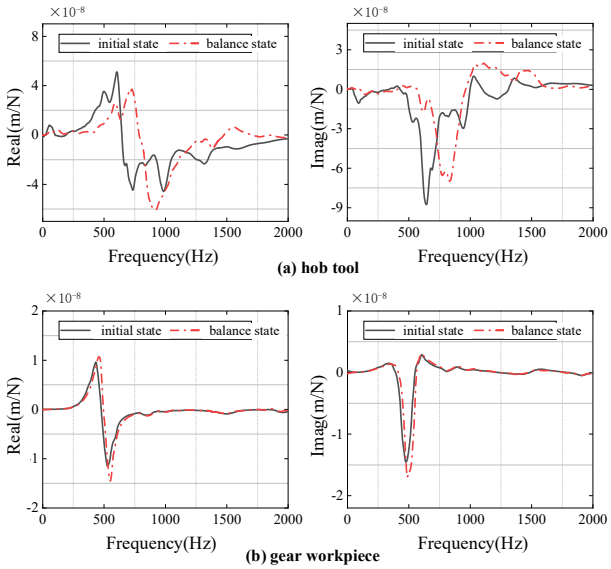

Figure 2. The measured FRFs

The peak extraction method is further used to extract the first three modal parameters from the hob frequency response function, as shown in Table 1. From the table, it can be seen that from the initial state to the thermal equilibrium state, the natural frequency and modal stiffness of the spindle system at the hob significantly increase, and the damping ratio shows a downward trend. The main reason is that with the increase of the temperature of the spindle, the preload force of the spindle bearing and other joints increases, resulting in an increase in the overall stiffness, and then changes the natural frequency and damping characteristics [16] of the spindle system. In addition, the changes of the second order natural frequency and modal stiffness are significantly lower than the changes of the first and third order. In summary, the time- varying thermal effect in the process of high-speed dry hobbing has a significant impact on the modal parameters of the hob spindle system. In order to construct the cutting stability boundary of hobbing under the time-varying thermal effect, it is necessary to study the evolution behavior of the dynamic characteristics of the spindle system under the time- varying thermal effect in the process of high-speed dry hobbing, and then build a modal parameter prediction model related to time-varying temperature.

Table 1. The modal parameters of the hob

The Modal parameters	Initial state values	Thermal balance state value	The value of the change
$f1$	664.52Hz	772.16	107.64
$f2$	954.75	958.42	3.67
$f3$	1212.75	1281	68.25
ξ_1	11.10	10.32	0.78
ξ_2	5.66	4.41	1.25
ξ_3	5.86	5.71	0.15
$K1$	5.73	9.9	4.17
$K2$	1.41	2.28	0.87
$K3$	1.92	3.37	1.45

f - natural frequency (Hz), ξ - damping ratio (%), K - modal stiffness ($\times 10^8$ N/m)

The temperature change of the measured point of the spindle system in the continuous machining process of high-speed dry hobbing is shown in Fig. 3. As can be seen from the figure, the temperature of the spindle system gradually increases with the hobbing process, and after a period of time, the temperature rise rate slows down and remains relatively stable. After the machining, the temperature of the spindle system decreases rapidly.

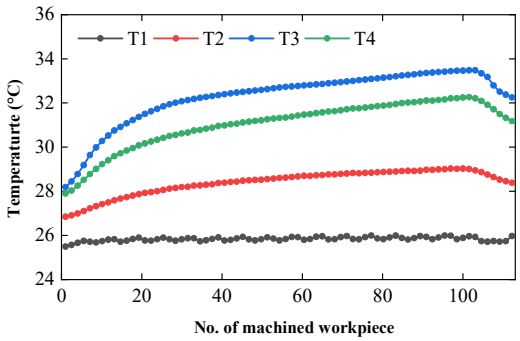

Figure 3. Temperature measurements

In order to extract the modal parameters of the spindle system during high-speed dry hobbing, the operating modal analysis method [20] based on Covariance-random subspace (COV-SSI) was adopted in this paper. First, the free vibration signals during the acceleration/deceleration stage of the spindle were extracted from the vibration signals of the spindle, as shown in Fig 4 (a). The modal parameters (natural frequency and damping ratio) at the measuring point of the spindle were estimated by COV- SSI, as shown in Fig. 4 (b). With this method, modal parameters are extracted once for every two workpieces processed from the collected signal data, a total of 50 groups are extracted.

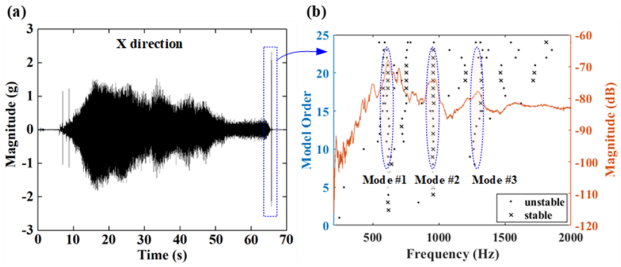

Figure 4. The COV-SSI based OMA

By comparing the measured vibration data, the modal parameters were extracted from the free vibration signal of the hob spindle (A2) in the X direction, as shown in Fig. 5, and the influence rule of time-varying thermal effect on the modal parameters during high-speed dry hobbing was analyzed. As can be seen from Fig. 5 (a), the natural frequency of the first and third modes increases significantly with the increase of the temperature of the spindle system, while the natural frequency of the second mode is less affected by the time-varying temperature. However, the damping ratio of the first three modes decreases with the increase of temperature, as shown in Fig. 5 (b). By comparing the results of the impact mode experiment and the operation mode experiment, it can

be seen that the modal parameters of the spindle system at the spindle head have the same changing trend as those at the hob. In view of this, this paper mainly predicts the modal parameters at the spindle head, so as to reveal the mapping relationship between the systematic dynamic characteristics of the spindle system and the time-varying temperature.

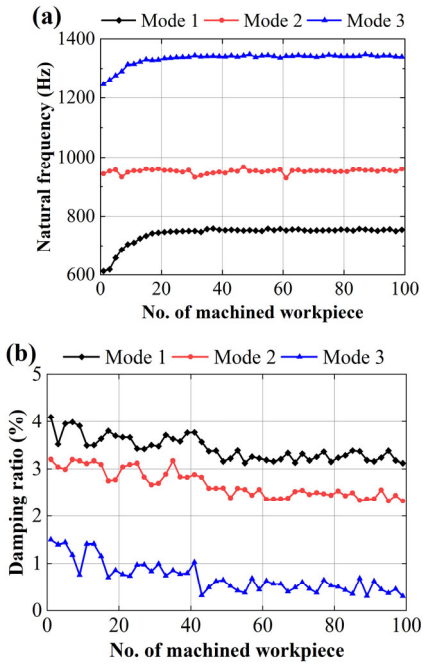

Figure 5. Evolution of the natural frequencies and damping ratios with machine tool thermal growth

4. Prediction Model of Spindle Modal Parameters Based on MOGPR

Assume that the temperature measurement value the spindle system at time i is $\mathbf{x}_i = \left(T_i^1, T_i^2, \ldots, T_i^m\right)$, m represents the number of temperature points being measured. The modal parameters at the corresponding time are. Where $\mathbf{y}_i = \left(y_i^1, y_i^2, \ldots, y_i^d\right)$ represents the number of multi-order modal parameters. If the time series for each temperature variable has n samples, then the input and output of the prediction model can be represented as sum, respectively $\mathbf{X}_{n\times m} = \left(\mathbf{x}_1, \mathbf{x}_2, \ldots, \mathbf{x}_n\right)^{\mathrm{T}}$ and $\mathbf{Y}_{n\times d} = \left(\mathbf{y}_1, \mathbf{y}_2, \ldots, \mathbf{y}_n\right)^{\mathrm{T}}$. Based on Gaussian process regression theory [21], the tth modal parameter can be represented by an unknown function containing noise.as shown in formula (1):

$$\mathbf{y}^t = f_t(\mathbf{x}) + \varepsilon_t, t = 1, 2, \ldots, d \tag{1}$$

In the formula, ε_t is the Gaussian prior noise considering the measurement error, obey $\varepsilon_t \sim N\left(0, \sigma_{s,t}^2\right)$, $f_t(\mathbf{x}) \sim \mathrm{GP}\left(0, k_t(\mathbf{x}, \mathbf{x}')\right)$ represents the nonlinear function with the Gaussian process prior, $k_t(\mathbf{x}, \mathbf{x}')$ is the covariance function, commonly expressed by the square exponential kernel function, as shown in formula (2).

$$k_t(\mathbf{x}, \mathbf{x}') = \sigma_{f,t}^2 \exp\left(-\frac{(\mathbf{x}-\mathbf{x}')^2}{2\sigma_q^2}\right) \tag{2}$$

Where $\sigma_{f,t}^2$ represents the variance of the data of the tth mode parameter, and σ_q^2 represents the correlation between the output temperature variables for the tth mode parameter.

Assuming that the output of the temperature related multi-modal parameter prediction model $\mathbf{f}(\mathbf{x}) = \left(f_1(\mathbf{x}), f_2(\mathbf{x}), \ldots, f_d(\mathbf{x})\right)$ also obeys the Gaussian process, it can be expressed as:

$$\mathbf{f}(\mathbf{x}) \sim \mathrm{GP}\left(\mathbf{0}, \mathbf{K}_{\mathrm{M}}(\mathbf{x}, \mathbf{x}')\right) \tag{3}$$

Where $\mathbf{K}_{\mathrm{M}}(\mathbf{x}, \mathbf{x}')$, denotes the multi-output covariance matrix, as shown in formula (4):

$$\mathbf{K}_{\mathrm{M}}(\mathbf{x}, \mathbf{x}') = \begin{bmatrix} k_{11}(\mathbf{x}, \mathbf{x}') & \cdots & k_{1d}(\mathbf{x}, \mathbf{x}') \\ \vdots & \ddots & \vdots \\ k_{d1}(\mathbf{x}, \mathbf{x}') & \cdots & k_{dd}(\mathbf{x}, \mathbf{x}') \end{bmatrix} \tag{4}$$

In the formula, $k_{t,t'}(\mathbf{x}, \mathbf{x}')$ represents the multi-output covariance function, which is used to reflect the correlation between the output of the tth mode parameter and the output of the t'th mode parameter.

To build a multi-output covariance function $k_{t,t'}(\mathbf{x}, \mathbf{x}')$, added $l^t = l$ to the prediction model as a variable to specify modal parameters. Then the multi-output covariance function [22], can be expressed as formula (5).

$$k_{\mathrm{M}}(\mathbf{x}, \mathbf{x}') = k_c(l, l') \times k_t(\mathbf{x}, \mathbf{x}') \tag{5}$$

In the formula, $k_c(l, l')$ used to indicate the correlation between any two modal parameters.

Therefore, the multi-output covariance matrix (formula (4)) in the multi-order modal parameter prediction model can be rewritten as formula (6)

$$\mathbf{K}_{\mathrm{M}}(\mathbf{X}, \mathbf{l}, \boldsymbol{\theta}_c, \boldsymbol{\theta}_t) = \mathbf{K}_c(\mathbf{l}, \boldsymbol{\theta}_c) \otimes \mathbf{K}_t(\mathbf{X}, \boldsymbol{\theta}_t) \tag{6}$$

In the formula, $\otimes$ is the Kronecker product, and $\mathbf{K}_c$ is the semi-positive definite covariance matrix of d*d dimensions, which can be constructed from the parameterized lower triangular matrix $\mathbf{L}$, as shown in formula (7)

$$\mathbf{K}_c = \mathbf{L}\mathbf{L}^T, \mathbf{L} = \begin{bmatrix} \theta_{c,1} & 0 & \cdots & 0 \\ \theta_{c,2} & \theta_{c,3} & \cdots & 0 \\ \vdots & \vdots & \ddots & \vdots \\ \theta_{c,p-d+1} & \theta_{c,p-d+2} & \cdots & \theta_{c,p} \end{bmatrix} \tag{7}$$

where $p = d \times (d+1)/2$ indicates the number of the hyper-parameters of K_c. The diagonal elements of the K_c represent the self-correlation of the modal parameters and the non-diagonal elements describe the correlation between different modal parameters.

After completing the training of the MOGPR model, for new model inputs $\{\mathbf{x}_*, \mathbf{l}_*\}$, the predicted values of the modal parameters can be obtained by calculating the posterior distribution, as shown in formula (8), Where, the posterior

mean and variance are shown in formula (9) respectively.

$$\mathbf{f}_*\left|\mathbf{X},\mathbf{l},\mathbf{Y},\mathbf{x}_*,\mathbf{l}_*\right. \sim N\left(\overline{\mathbf{f}}_*(\mathbf{x}_*),\operatorname{cov}\mathbf{f}_*\right) \tag{8}$$

$$\begin{aligned}\overline{\mathbf{f}}_* &= \mathbf{K}_{\mathrm{M}}(\mathbf{x}_*,\mathbf{X})\left[\mathbf{K}_{\mathrm{M}}(\mathbf{X},\mathbf{X})+\boldsymbol{\Sigma}_{\mathrm{M}}\right]^{-1}\mathbf{Y}\\ \operatorname{cov}\mathbf{f}_* &= \mathbf{K}_{\mathrm{M}}(\mathbf{x}_*,\mathbf{x}_*)-\\ &\quad \mathbf{K}_{\mathrm{M}}(\mathbf{x}_*,\mathbf{X})\left[\mathbf{K}_{\mathrm{M}}(\mathbf{X},\mathbf{X})+\boldsymbol{\Sigma}_{\mathrm{M}}\right]^{-1}\mathbf{K}_{\mathrm{M}}(\mathbf{X},\mathbf{x}_*)\end{aligned} \tag{9}$$

Where $\boldsymbol{\Sigma}_{\mathrm{M}}=\operatorname{diag}(\sigma_{s,1}^2,\sigma_{s,2}^2,\ldots,\sigma_{s,d}^2)\otimes\mathbf{I}_n$ is diagonal noise matrix.

In order to predict multi-order modal parameters simultaneously, it is necessary to solve for the hyperparameters in the multi-output covariance matrix. which can be obtained by minimizing the negative log marginal likelihood (NLML), as shown in formula (10).

$$\begin{aligned}\boldsymbol{\theta}_{\mathrm{M,opt}} &= \underset{\boldsymbol{\theta}_{\mathrm{M}}}{\operatorname{argmin}}\left\{-\log p\left(\mathbf{Y}\left|\mathbf{X},\boldsymbol{\theta}_{\mathrm{M}}\right.\right)\right\}\\ &= \operatorname{argmin}\frac{1}{2}\left\{\begin{array}{l}\mathbf{Y}^{\mathrm{T}}\left(\mathbf{K}_{\mathrm{M}}+\boldsymbol{\Sigma}_{\mathrm{M}}\right)^{-1}\mathbf{Y}+\\ \log\left|\mathbf{K}_{\mathrm{M}}+\boldsymbol{\Sigma}_{\mathrm{M}}\right|+n\log 2\pi\end{array}\right.\end{aligned} \tag{10}$$

Based on references [23], the hyperparameters in formula (10) can be solved by using gradient descent algorithm to solve the partial derivative of marginal likelihood function. In order to evaluate the accuracy of the MOGPR prediction model, the root-mean-square error (RMSE) and determination coefficient (R^2) were used in this paper to calculate the accuracy of the MOGPR model in the training and test datasets [24], as shown in formulas (11) and (12), where the smaller the RMSE value and the larger the R^2 value, the higher the accuracy of the prediction model.

$$\mathrm{RMSE}=\sqrt{\frac{1}{n}\sum_{i=1}^{n}\left(y_i^t-\hat{y}_i^t\right)^2} \tag{11}$$

$$R^2=\frac{\left[\sum_{i=1}^{n}\left(y_i^t-\overline{y}^t\right)\left(\hat{y}_i^t-\overline{\hat{y}}^t\right)\right]^2}{\sum_{i=1}^{n}\left(y_i^t-\overline{y}^t\right)^2\sum_{i=1}^{n}\left(\hat{y}_i^t-\overline{\hat{y}}^t\right)^2} \tag{12}$$

where y_i^t and $\hat{y}_i^t$ denote the ith measured and predicted values for the tth modal parameter, respectively, $\overline{y}^t$ and $\overline{\hat{y}}^t$ are the means of the measured and predicted values for the tth modal parameter, respectively.

5. Analysis of Prediction Results of MOGPR Model

Based on the results of operation modal experiments, a total of 50 datasets were constructed, and each dataset contained the natural frequency (f_1, f_2, f_3) and damping ratio (ξ_1, ξ_2, ξ_3) of the first three modes, as well as the temperature of the four measured points on the spindle (T1, T2, T3, T4). The 50 datasets were divided into training datasets and test datasets by quintuple cross-validation method, that is, 40 datasets were used for model training, and the remaining 10 datasets were used for model testing and verification. The training accuracy of the MOGPR model is shown in Fig 6. It can be seen from the figure that the prediction index R^2 of the first three order natural frequency and the second order damping ratio is close to 1, while the R^2 of the first and third order damping ratio is also higher than 0.8 and the RMSE value is small, indicating that the MOGPR model has a high prediction accuracy.

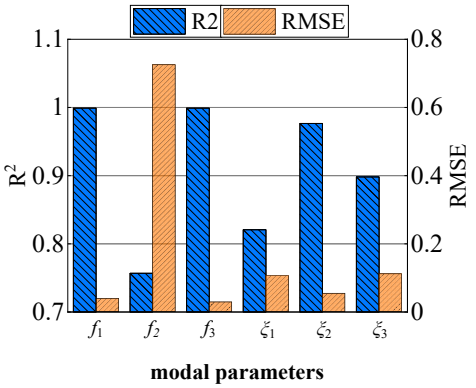

Figure 6. The prediction accuracy of the MOGPR model

Ten sets of test data were utilized to assess and validate the trained MOGPR model. A comparison between the predicted values derived from the MOGPR model and the actual measured values from the test data set is depicted in Fig. 7. In this figure, RE signifies the relative error between the measured and predicted values. It is evident from the figure that the relative error associated with the damping ratio is generally higher compared to that of the natural frequency. Furthermore, aside from the third-order damping ratio, which exhibits a relatively significant error, the relative errors for the remaining damping ratios are below 15%. Overall, the trained MOGPR model demonstrates efficient and accurate prediction capabilities for temperature-related modal parameters of the spindle system.

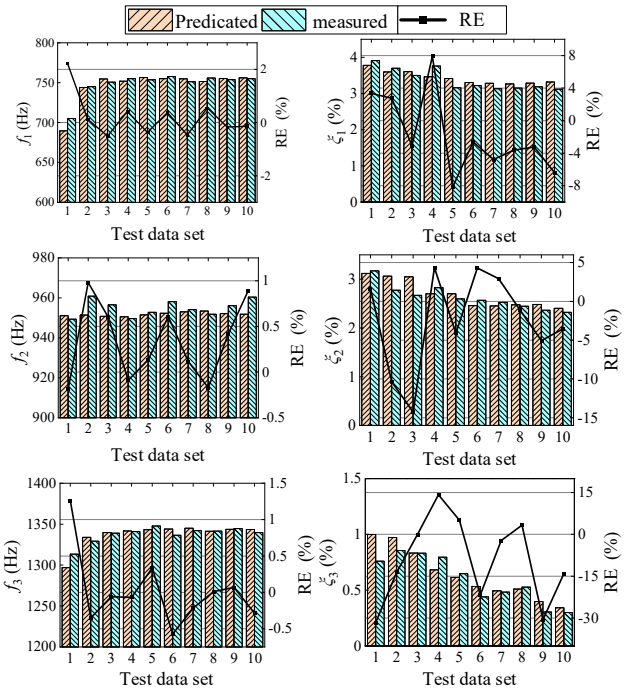

Figure 7. Validation of the prediction model

6. Conclusion

During the high-speed dry hobbing process, the dynamic characteristics of the machine tool are particularly sensitive to time-varying thermal effects. To ensure high stability and optimal performance in high-speed dry hobbing, accurate prediction of these characteristics is paramount. Through impact and operation mode experiments, a comprehensive analysis of the spindle system's modal parameters under varying thermal conditions was conducted. The results indicate that with increasing temperature, the natural frequency and modal stiffness of the spindle system enhance, whereas the damping ratio diminishes. Using experimental data from the high-speed dry hobbing process, a temperature-dependent modal parameter prediction model for the spindle system was established using MOGPR, and its predictive accuracy was rigorously tested. This established MOGPR model offers reliable predictions of temperature-related modal parameters, paving the way for further exploration of cutting stability boundaries influenced by time-varying temperatures.

Acknowledgment

Greatly appreciated to Chongqing Technology and Business University for providing valuable machine tool support for the experimental research work presented in this paper.

References

[1] Cao Huajun, Li Xianguang, Chen Peng. The Theory and Key Technology of Green high-speed dry hobbing Process [M]. Chongqing: Chongqing University Press, 2016: 2-7.

[2] CAO H, ZHU L, LI X, et al. Thermal error compensation of dry hobbing machine tool considering workpiece thermal deformation [J]. International Journal of Advanced Manufacturing Technology, 2016, 86(5-8): 1-13.

[3] MAYR J, JEDRZEJEWSKI J, UHLMANN E, et al. Thermal issues in machine tools [J]. CIRP Annals - Manufacturing Technology, 2012, 61(2): 771–91.

[4] ZAGHBANI I, SONGMENE V. Estimation of machine-tool dynamic parameters during machining operation through operational modal analysis [J]. Pergamon, 2009, (12).

[5] Yang Xiao, Cao Huajun, Chen Yongpeng, et al. Entire process transfer model of cutting heat in high-speed dry gear hobbing process system [J]. Journal of Mechanical Engineering, 2015, 51(19): 189-96.

[6] LI B, CAO H, YANG X, et al. Thermal energy balance control model of motorized spindle system enabling high-speed dry hobbing process [J]. Journal of Manufacturing Processes, 2018, 35(OCT.): 29-39.

[7] ZHU X L, BENJIE. Multi-variable driving thermal energy control model of dry hobbing machine tool [J]. The International Journal of Advanced Manufacturing Technology, 2017, 92(1a4).

[8] YANG X, CAO H, LI B, et al. A thermal energy balance optimization model of cutting space enabling environmentally benign dry hobbing - ScienceDirect [J]. Journal of Cleaner Production, 2018, 172: 2323-35.

[9] GE Z D, XIAOHONG. Thermal error control method based on thermal deformation balance principle for the precision parts of machine tools [J]. The International Journal of Advanced Manufacturing Technology, 2018, 97(1a4).

[10] ABELE E, ALTINTAS Y, BRECHER C. Machine tool spindle units [J]. CIRP Annals - Manufacturing Technology, 2010, 59(2): 781-802.

[11] MA C, YANG J, ZHAO L, et al. Simulation and experimental study on the thermally induced deformations of high-speed spindle system [J]. Appl Therm Eng, 2015, 86: 251-68.

[12] Yan Zongzhuo, Tao Tao, Hou Ruisheng, et al. Research on convolution modeling of thermal characteristics of machine tool spindle [J]. Journal of Xi'an Jiaotong University, 2019, 53(6): 1-9.

[13] GE Z, DING X. Design of thermal error control system for high-speed motorized spindle based on thermal contraction of CFRP [J]. Int J Mach Tools Manuf, 2018, 125: 99-111.

[14] GRAMA S N, MATHUR A, BADHE A N. A model-based cooling strategy for motorized spindle to reduce thermal errors [J]. Int J Mach Tool Manu, 2018, 132: 3-16.

[15] ZHENG D, CHEN W. Thermal performances on angular contact ball bearing of high-speed spindle considering structural constraints under oil-air lubrication [J]. Tribology International, 2017, 109: 593-601.

[16] LI B, CHEN Y, YANG X, et al. Influence of thermal effect on dynamic behavior of high-speed dry hobbing motorized spindle system [J]. Journal of Mechanical Science and Technology, 2022, (5): 36.

[17] ZHANG, YANFEI, LI, et al. Uneven heat generation and thermal performance of spindle bearings [J]. Tribology International, 2018.

[18] STEIN J L, TU J F. A State-Space Model for Monitoring Thermally Induced Preload in Anti-Friction Spindle Bearings of High-Speed Machine Tools [J]. Journal of Dynamic Systems Measurement & Control, 1994, 116(3): 372-86.

[19] LIN C W, TU J, KAMMAN J. An integrated thermo-mechanical-dynamic model to characterize motorized machine tool spindles during very high speed rotation [J]. International Journal of Machine Tools & Manufacture, 2003, 43: 1035-50.

[20] LI B, LI L, HE H, et al. Research on modal analysis method of CNC machine tool based on operational impact excitation [J]. The International Journal of Advanced Manufacturing Technology, 2019.

[21] LIU H, CAI J, ONG Y S. Remarks on multi-output Gaussian process regression [J]. Knowledge-Based Systems, 2017, 144(mar.15): 102-21.

[22] LEI Y, HOU T, DING Y. Prediction of the Posture-Dependent Tool Tip Dynamics in Robotic Milling Based on Multi-Task Gaussian Process Regressions [J]. Robotics and Computer Integrated Manufacturing, 2023.

[23] ZHOU P, XU Z, PENG X, et al. Long-term prediction enhancement based on multi-output Gaussian process regression integrated with production plans for oxygen supply network [J]. Comput Chem Eng, 2022, 163: 107844.

[24] CHEN B, SHEN L, ZHANG H. A hybrid proper orthogonal decomposition-heteroscedastic sparse Gaussian process regression model for evaluating structural reliability with correlated stochastic material properties [J]. Structural safety, 2023.